Catalysis Today xxx (xxxx) xxx–xxx

Contents lists available at ScienceDirect

Catalysis Today

journal homepage: www.elsevier.com/locate/cattod

Degradation of herbicide S-metolachlor by electrochemical AOPs using a boron-doped diamond anode

Diego Roberto Vieira Guelfi[a,b], Fábio Gozzi[a], Amílcar Machulek Jr.[a], Ignasi Sirés[b,*], Enric Brillas[b], Silvio C. de Oliveira[a,*]

[a] Instituto de Química (INQUI), Universidade Federal de Mato Grosso do Sul, Av. Senador Filinto Muller, 1555, CP 549, MS 79074-460 Campo Grande, Brazil
[b] Laboratori d'Electroquímica dels Materials i del Medi Ambient, Departament de Química Física, Facultat de Química, Universitat de Barcelona, c/Martí i Franquès 1-11, 08028 Barcelona, Spain

ARTICLE INFO

Keywords:
Boron-doped diamond anode
Electro-Fenton
Electro-oxidation
Photoelectro-Fenton
S-metolachlor
Water treatment

ABSTRACT

The degradation and mineralization ability of electrochemical processes like electro-oxidation with electrogenerated H_2O_2 (EO-H_2O_2), electro-Fenton (EF) and UVA-assisted photoelectro-Fenton (PEF) has been comparatively studied for solutions of the herbicide S-metolachlor. Solutions of 100 mL have been treated using an undivided cell equipped with an air-diffusion cathode and a boron-doped diamond (BDD) anode. The effect of pH, current density, and Fe^{2+} and S-metolachlor concentrations has been thoroughly studied. The total organic carbon removal profiles have demonstrated the feasibility of almost overall mineralization by EF and PEF after 9 h at 300 mA. The herbicide decays in both treatments informed about the complexation of Fe(III) ions formed from Fenton's reaction, which decelerated S-metolachlor removal. However, the high oxidation power of BDD anode allowed the gradual mineralization of such complexes. The identification of chlorinated and non-chlorinated degradation byproducts by GC–MS has allowed the proposal of main degradation routes.

1. Introduction

The large consumption of herbicides worldwide contributes in a very significant manner to environment contamination and, as a result, public health is currently at stake [1]. The herbicide S-metolachlor (ST, $C_{15}H_{22}ClNO_2$, 2-chloro-*N*-(2-ethyl-6-methylphenyl)-*N*-[(1S)-2-methoxy-1-methylethyl]acetamide) is a selective chloroacetanilide herbicide that has been applied since the 1970s to more than 70 different crops to control small leaf weeds in the pre and post-emergence period [2]. Its high water solubility (480 mg L^{-1} at 20 °C), low vapor pressure (1.73×10^{-3} Pa at 20 °C) and large half-life owing to its slow degradation by photolysis (70 days exposure to sunlight) or hydrolysis (30 days at pH 5–9) led to classify S-metolachlor residues as persistent [3,4]. Its large usage and relatively low adsorption in soil cause a considerable discharge into groundwater, thus compromising water quality [5]. Although ST is classified as moderately toxic (Class III) [4,6], its negative impact on aquatic microorganisms like phytoplankton [7], fish [8] and crustaceans [9], as well as on certain types of human cells [10] has been reported. Several authors have investigated the performance of various methods to treat water containing this and other herbicides. TiO_2 photocatalysis [11], photo-Fenton with artificial and natural light [12,13], electro-Fenton (EF) [14–20], and UVA- or solar-assisted photoelectro-Fenton (PEF) with in situ H_2O_2 electrogeneration [16,20–22] have yielded very positive results.

The electrochemical advanced oxidation processes (EAOPs) like electro-oxidation with electrogenerated H_2O_2 (EO-H_2O_2), EF and PEF have been progressively receiving increasing interest for the removal of toxic organic contaminants from water due to their great performance, in combination with simple setups, safe procedures and affordable costs [23–28]. They promote the oxidation of organic compounds upon in situ generation of hydroxyl radical (·OH), which exhibits a high redox potential (E° = 2.8 V/SHE), yielding a high degree of mineralization [29–32].

In EO, which is the most widely employed EAOP, the formation of physisorbed ·OH (M(·OH)) occurs at the surface (M) of a non-active anode such as boron-doped diamond (BDD) from water oxidation at high applied current or potential, as shown in reaction (1) [30]. BDD is the most effective anode among those tested so far, having demonstrated its effectiveness also for the total degradation of herbicide residues [18,30]. Apart from its large overpotential for O_2 evolution and low adsorption of any species including ·OH, BDD presents very appealing technological properties such as a high mechanical, thermal and chemical resistance [32].

* Corresponding authors.
E-mail addresses: i.sires@ub.edu (I. Sirés), scolive@gmail.com (S.C. de Oliveira).

http://dx.doi.org/10.1016/j.cattod.2017.10.026
Received 14 August 2017; Received in revised form 17 October 2017; Accepted 24 October 2017

$$M + H_2O \rightarrow M(^{\bullet}OH) + H^+ + e^- \quad (1)$$

The EO process can be combined with the cathodic electrogeneration of H_2O_2, yielding the so-called EO-H_2O_2. Several kinds of carbonaceous materials have been used for this purpose, being carbon-PTFE-based air-diffusion cathodes especially useful because of their large ability to favor the two-electron reduction of gaseous O_2 from reaction (2):

$$O_{2(g)} + 2H^+ + 2e^- \rightarrow H_2O_2 \quad (2)$$

Additional amounts of ·OH in bulk solution can be generated in EF from the catalytic decomposition of H_2O_2 by Fe^{2+} at pH 3.0, following Fenton's reaction (3). The catalytic cycle can be maintained since Fe^{3+} can be reduced at the cathode to regenerate Fe^{2+} via reaction (4) [29]. The oxidation ability of EF process can be enhanced upon irradiation with UVA light (λ_{max} = 360 nm), yielding the so-called PEF process, which promotes the photoreduction of Fe(III) species from reaction (5), giving rise to additional amounts of ·OH, and the photodecomposition of Fe(III)-carboxylate complexes from reaction (6) [29–32]. Note that H_2O_2 is not photolyzed to ·OH radical because this would require higher energy such as that provided by UVC light (λ_{max} = 254 nm) [29].

$$H_2O_2 + Fe^{2+} \rightarrow Fe^{3+} + {}^{\bullet}OH + OH^- \quad (3)$$

$$Fe^{3+} + e^- \rightarrow Fe^{2+} \quad (4)$$

$$Fe(OH)^{2+} + h\nu \rightarrow Fe^{2+} + {}^{\bullet}OH \quad (5)$$

$$Fe(OOCR)^{2+} + h\nu \rightarrow Fe^{2+} + CO_2 + R^{\bullet} \quad (6)$$

Aiming to evaluate the comparative performance of EO-H_2O_2, EF and PEF to degrade the herbicide S-metolachlor, this paper presents a thorough investigation on the behavior of ST solutions treated in an undivided BDD/air-diffusion cell. The effect of pH on the oxidation ability of EO-H_2O_2 was studied. The influence of the applied current, and the Fe^{2+} and ST concentrations in EF was assessed from total organic carbon (TOC) and high-performance liquid chromatography (HPLC) measurements. The main reaction byproducts were identified by gas chromatography-mass spectrometry (GC–MS).

2. Material and methods

2.1. Chemicals

S-metolachlor (Pestanal®) with purity > 98% was obtained from Sigma-Aldrich. Vetec Quimica Fina supplied the $Fe_2SO_4{\cdot}7H_2O$, Na_2SO_4 and concentrated H_2SO_4. A Gehaka DG500 UF system was employed to produce pure water (resistivity > 18 MΩ cm) needed to prepare all solutions to be degraded. Other chemicals used in various analytical techniques were obtained from J.T. Baker and Vetec Quimica Fina.

2.2. Electrolytic system

Comparative treatments of 100 mL of ST solutions with 0.050 M Na_2SO_4 were carried out by EO-H_2O_2, EF and PEF using an open, undivided glass cell (capacity of 150 mL) with a jacket for recirculation of water at 25 °C. During the trials, solutions were stirred using a magnetic follower. All details on the power source employed to operate galvanostatically and the UVA lamp to irradiate the solutions in PEF can be found elsewhere [20,33]. The BDD anode and carbon-PTFE air-diffusion cathode (3 cm^2 each) used in all the experiments, conveniently cleaned and activate prior to first use [20], were purchased from NeoCoat and E-TEK, respectively. In order to ensure the H_2O_2 production along the electrolyses, the cathode was connected to an air pump (flow rate of 1 L min^{-1}). It must be noted that the use of such a small electrolytic system limits the current efficiency of electrode reactions, particularly the ST removal with BDD($^{\bullet}OH$) that is controlled by the mass transport of organic pollutants.

2.3. Instruments and analytical procedures

The degradation of ST was monitored by HPLC using a Thermo Scientific Finnigan chromatograph equipped with: (i) an autosampler, (ii) a photodiode array detector (set a constant wavelength of 215 nm), and (iii) a 5 µm Agilent Technologies Zorbax Eclipse XDB-C-18 column (250 mm × 4.6 mm). The mobile phase consisted in a 40:60 (v/v) H_2O/CH_3CN mixture eluted at a flow rate of 0.6 mL min^{-1}. At selected treatment times, samples were collected, immediately diluted with CH_3CN and then filtered (0.45 µm PTFE filters). Chloride, chlorate, ammonium and nitrate ions were quantified following standard procedures [34,35]. The pH monitoring, TOC analysis and calculation of mineralization current efficiency (MCE) for each assay were performed as described in previous studies [20,36]. The number of electrons *n* involved in the theoretical global mineralization process of ST was 74 according to reaction (7), which considers the quantitative formation of ammonium (95% of initial N was accumulated as NH_4^+ and 5% as NO_3^-) and chloride ions (subsequently transformed into chlorate ions).

$$C_{15}H_{22}ClNO_2 + 28H_2O \rightarrow 15CO_2 + NH_4^+ + Cl^- + 74H^+ + 74e^- \quad (7)$$

Worth mentioning, the MCE is an average value that considers globally the organic matter to be mineralized, thus ignoring the particular role of reaction intermediates which have variable oxidation state of carbon.

The main byproducts formed upon treatment of 100 mL of ST solutions by EAOPs were identified by GC–MS using a NIST05-MS library. For this, the samples were treated by liquid-liquid extraction method using $C_2H_2Cl_2$ [20]. GC–MS analysis was made with an Agilent Technologies system composed of a 6890N GC, fitted with a nonpolar Teknokroma Sapiens-X5MS or polar Agilent 19091N-133 HP Innowax column, and a 5975C MS operating in electron impact mode at 70 eV. The temperature ramp was: 36 °C for 1 min, 5 °C min^{-1} up to 250 °C (polar) or 320 °C (non-polar) and hold time 10 min. The temperature of the inlet, source and transfer line was 250, 230 and 250–300 °C, respectively.

3. Results and discussion

3.1. Effect of initial pH on the EO-H_2O_2 treatment

For some pollutants, the initial pH is an important parameter in the EO-H_2O_2 treatment because it may affect the protonation/deprotonation equilibria and various reactions where protons have a role, including for example the adsorption of the molecule on the electrodes. Solutions with 0.28 mM ST and 0.050 M Na_2SO_4 were treated at initial pH of 3.0, 5.0 or 9.0 at 300 mA for 540 min. The ST concentration decay shown in Fig. 1a highlights its total disappearance thanks to the oxidation by BDD(·OH), requiring 240 min at pH 3.0 and 5.0 and 360 min at pH 9.0. Nevertheless, the degradation was slighly faster at pH 3.0, which can be explained, at least in part, by the higher concentration of protons that favored the cathodic formation of H_2O_2 from reaction (2) [37]. This suggests a certain contribution of H_2O_2 to the oxidative degradation of ST. The slighly slower ST decay at pH 9.0 could also be related to the competitive oxidation of OH^- to O_2 at BDD without production of hydroxyl radicals [38], which causes a lower generation of BDD($^{\bullet}OH$) from reaction (1). The inset panel of Fig. 1a presents the good fitting obtained from a pseudo-first-order kinetic analysis of the previous decays for the first 30 min, yielding apparent rate constant (k_{app}) values of 0.014, 0.010 and 0.011 min^{-1} at pH 3.0, 5.0 and 9.0, respectively (see Table 1).

Fig. 1b shows no substantial difference between the TOC removals achieved in EO-H_2O_2 at those three pH values until 6 h of electrolysis, which agrees with the behavior of another herbicide like mecoprop [21]. At 9 h, however, the mineralization attained was 96% at pH 3.0,

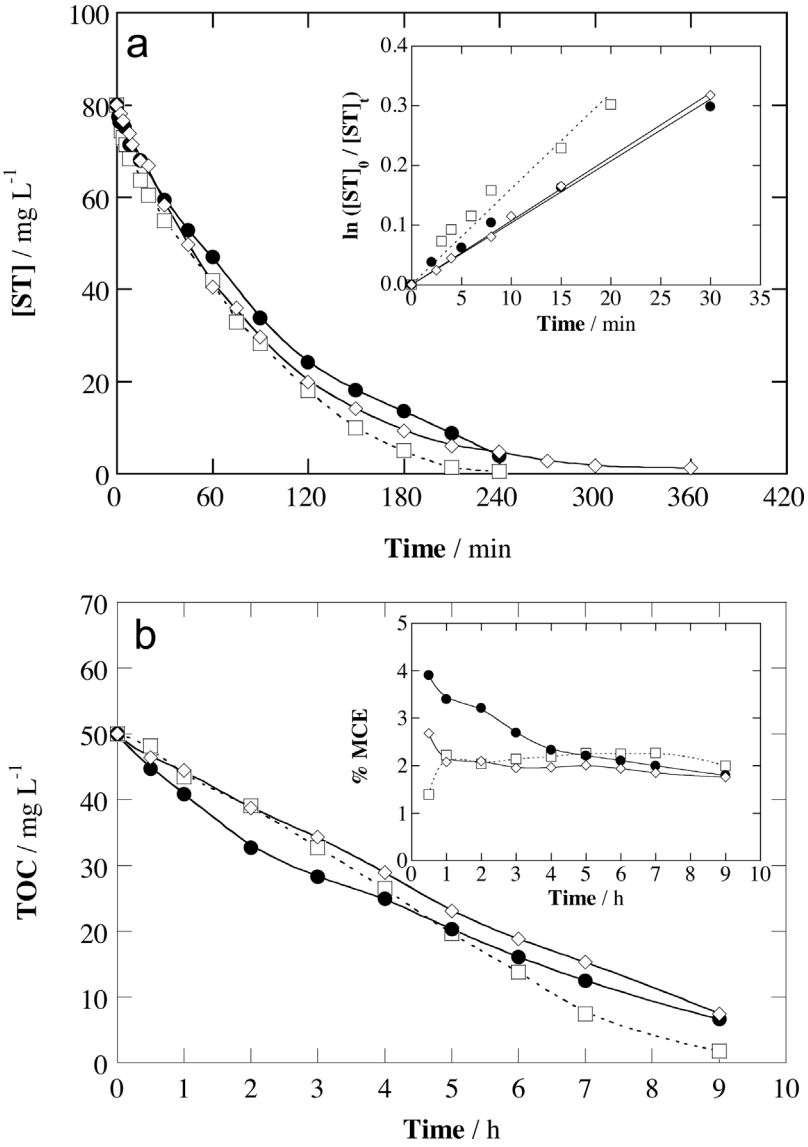

Fig. 1. (a) Concentration decay, (a, inset) kinetic analysis considering a pseudo-first-order reaction, (b) TOC removal and (b, inset) mineralization current efficiency versus time obtained for the electrochemical oxidation with electrogenerated H_2O_2 (EO-H_2O_2) of 100 mL of 0.28 mM S-metolachlor (ST) solutions in 0.050 M Na_2SO_4 using a stirred BDD/air-diffusion cell at 300 mA and 25 °C. Initial pH: (□) 3.0, (●) 5.0 and (◊) 9.0.

Table 1
Apparent rate constants and *R*-squared for the degradation of herbicide S-metolachlor solutions of 100 mL with 0.050 M Na_2SO_4 by EAOPs using a stirred BDD/air-diffusion cell at 25 °C.

Method	[ST] (mg L^{-1})	pH	*I* (mA)	[Fe^{2+}] (mM)	$k_{app,1}$ (min^{-1})	R^2	$k_{app,2}$ (min^{-1})	R^2
EO-H_2O_2	80	3.0	300	–	0.014	0.979	–	–
EO-H_2O_2	80	5.0	300	–	0.010	0.983	–	–
EO-H_2O_2	80	9.0	300	–	0.011	0.999	–	–
EF	80	3.0	100	0.50	0.34	0.994	0.014	0.971
EF	80	3.0	200	0.50	0.26	0.993	0.014	0.992
EF	80	3.0	300	0.50	0.16	0.992	0.030	0.987
EF	80	3.0	300	0.10	0.043	0.996	0.011	0.973
EF	80	3.0	300	1.00	0.75	0.997	0.038	0.989
EF	80	3.0	300	1.50	0.45	0.981	0.063	0.979
EF	160	3.0	300	0.50	0.12	0.987	0.021	0.990
EF	40	3.0	300	0.50	0.53	0.998	0.091	0.996
PEF	80	3.0	300	0.50	0.35	0.992	0.048	0.997

being greater than 86% found at pH 5.0 and 9.0. The inset panel of Fig. 1b depicts the corresponding time course of MCE during the treatments, reaching very low values (< 4%). This evidences that EO-H_2O_2 is a rather inefficient process due to the mass transport limitations associated to the fact that the BDD(·OH) is confined to a small region of the cell and hence, EF was tested as an alternative.

3.2. Effect of applied current on the EF process

The applied current has a direct effect on both, the generation rate of BDD(·OH) at the anode surface from reaction (1) and that of H_2O_2 from reaction (2), which in turn affects the formation rate of free ·OH from Fenton's reaction (3). Solutions of 0.28 mM ST with 0.050 M Na_2SO_4 and 0.50 mM Fe^{2+} at pH 3.0 and 25 °C were treated by EF at current values from 100 to 300 mA.

As can be observed in Fig. 2a, the EF treatment at 300 mA required only 120 min to completely remove ST, being much quicker than EF at 100 and 200 mA (180 min) and EO-H_2O_2 (240 min, Fig. 1a). The faster decay in the presence of Fe^{2+} catalyst is mainly due to the formation of ·OH in the bulk, overcoming the abovementioned mass transport limitations since the ST molecules can encounter the radicals within the whole cell volume. Moreover, the increase of current from 100 to 300 mA promoted the gradually larger accumulation of radicals from reaction (1) and (3). The inset panel of Fig. 2a shows a quite different kinetic behavior compared to Fig. 1a. In the presence of Fe^{2+}, two consecutive regions associated to pseudo-first-order kinetics can be observed at all current values. The first region, from 0 to 5 min, presented a very fast ST decay due to the action of BDD(·OH) and, mainly,

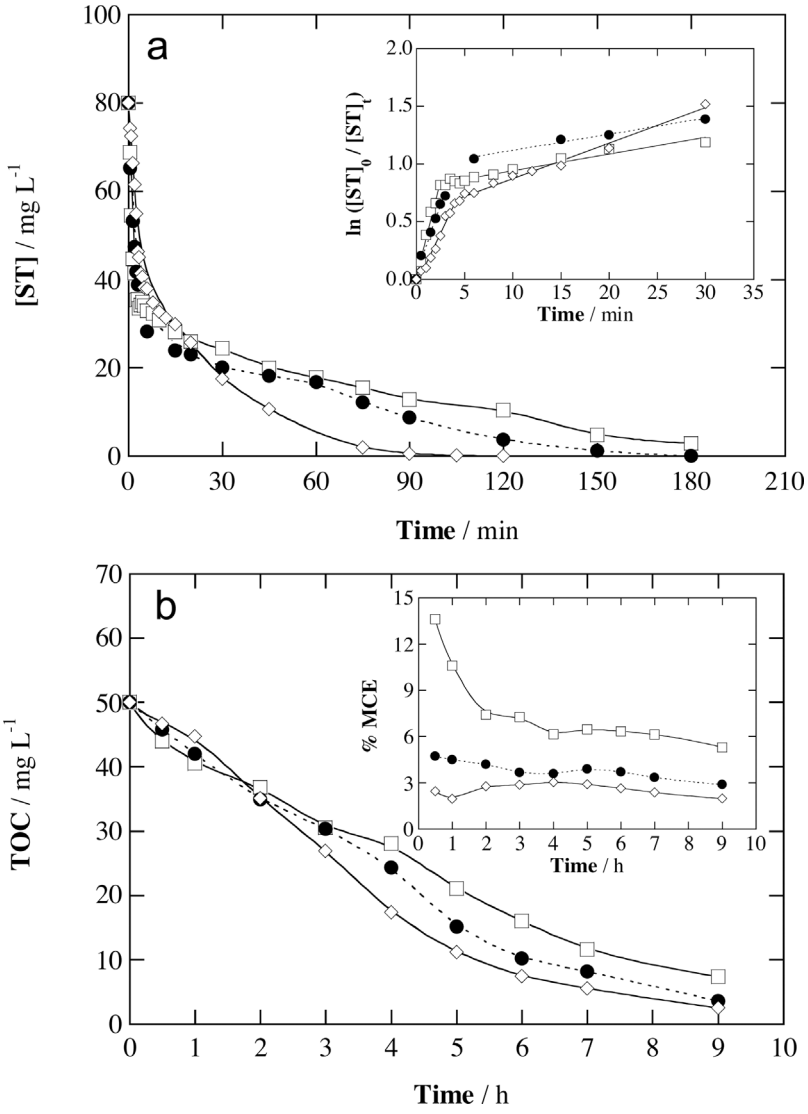

Fig. 2. (a) Concentration abatement, (a, inset) pseudo-first-order kinetics, (b) TOC decay and (b, inset) mineralization current efficiency versus time found for the electro-Fenton (EF) treatment of 100 mL of 0.28 mM ST solutions with 0.050 M Na_2SO_4 and 0.50 mM Fe^{2+} using a stirred BDD/air-diffusion cell at pH 3.0 and 25 °C. Applied current: (□) 100 mA, (●) 200 mA and (◊) 300 mA.

the ·OH produced from Fenton's reaction (3). The lower k_{app} obtained as the applied current was increased (Table 1) can be explained by the faster generation of certain byproducts that compete with ST to react with hydroxyl radicals. The second region, from 5 to 30 min, presented a much slower herbicide concentration decay, with a decrease of about one order of magnitude in the k_{app} values (Table 1). Note that these latter values were close to the k_{app} found in EO-H_2O_2. This kinetic behavior can be explained as follows: initially, iron ions are in the form of Fe^{2+}, which react with H_2O_2 via Fenton's reaction (3) and produce large amounts of ·OH; however, the regeneration of Fe^{2+} from reaction (4) is difficult [29], favoring the formation of complexes between Fe (III) and ST and hence, after 5 min of electrolysis these remaining complexes are mainly degraded only by BDD(·OH), as occurs in EO-H_2O_2. Therefore, the inflection point appears once the ST concentration is low enough so as to form Fe(III)-ST complexes to a large extent. The existence of two consecutive degradation regions related to the formation of Fe(III) complexes has also been reported for the EF treatment of another *N*-compound, i.e., the insecticide propoxur [20].

The TOC removals corresponding to the same trials are shown in Fig. 2b. As in the case of Fig. 1a, there was no remarkable difference within the first minutes of EF treatment. Conversely, the mineralization was much quicker from 2 to 3 h of treatment, attaining 85%, 93% and 95% after 9 h at 100, 200 and 300 mA, respectively. The superiority of the higher current values can be due to the favored Fe^{2+} regeneration with higher ·OH production in the bulk once ST has been totally removed. The inset depicts the MCE values, which attained 13% as maximal during the first minutes at 100 mA, and always became progressively lower as the current was raised. This can be accounted for by the greater extent of parasitic reactions (8)–(11) as current increases [29–32]. Reaction (8) is the most important side reaction since O_2 evolution is largely enhanced removing a larger proportion of BDD(·OH). The greater H_2O_2 production also reduces the ·OH concentration in the bulk via reaction (9) with generation of the weak hydroperoxyl radical (HO_2·). The quicker rise in O_3 and $S_2O_8^{2-}$ generation from electrode reactions (10) and (11) also inhibits the anodic production of BDD(•OH) from reaction (1).

$$2BDD(^{\bullet}OH) \rightarrow 2BDD + O_2 + 2H^+ + 2e^- \quad (8)$$

$$H_2O_2 + {}^{\bullet}OH \rightarrow HO_2^{\bullet} + H_2O \quad (9)$$

$$3H_2O \rightarrow O_3 + 6H^+ + 6e^- \quad (10)$$

$$2SO_4^{2-} \rightarrow S_2O_8^{2-} + 2e^- \quad (11)$$

3.3. Effect of initial Fe^{2+} concentration on the EF process

To assess the influence of the content of Fe^{2+} catalyst on the EF process, 0.28 mM ST solutions with 0.050 M Na_2SO_4 were treated at pH

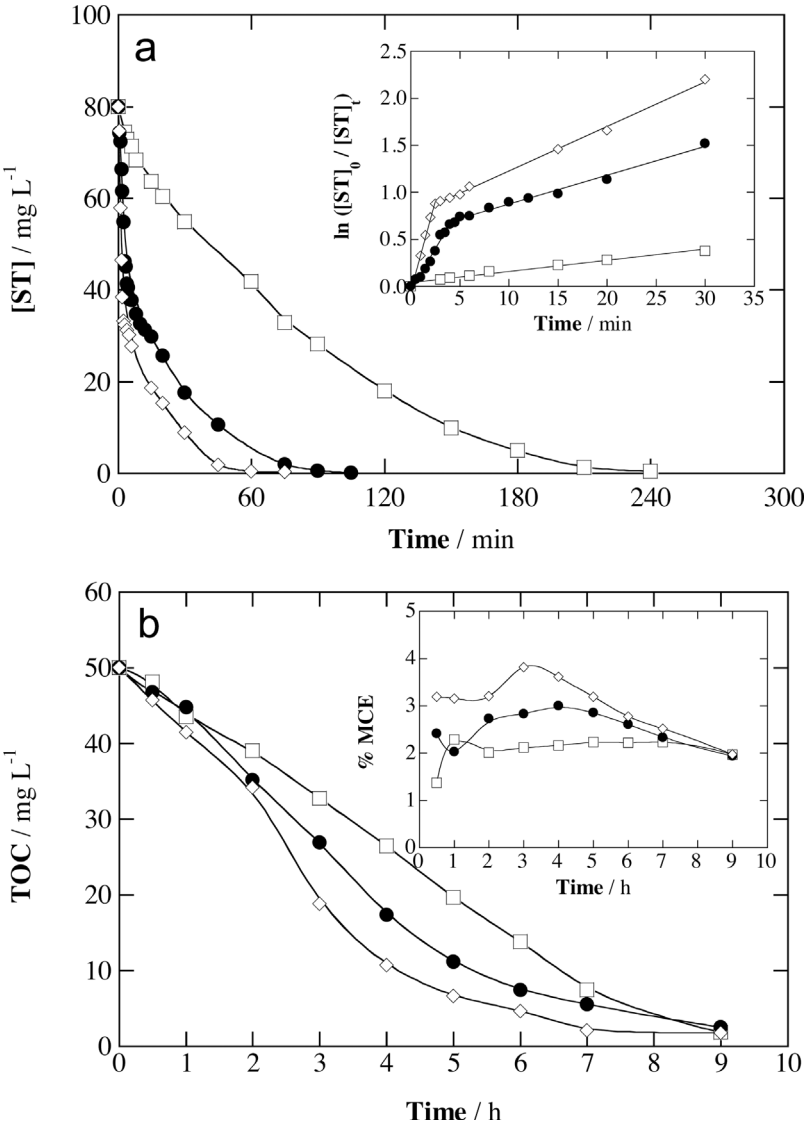

Fig. 3. (a) Concentration abatement, (a, inset) pseudo-first-order kinetics, (b) TOC reduction and (b, inset) mineralization current efficiency versus time determined for the treatment of 100 mL of 0.28 mM ST solutions with 0.050 M Na_2SO_4 at pH 3.0 using a stirred BDD/air-diffusion cell at 300 mA and 25 °C. Method: (□) EO–H_2O_2, (●) EF with 0.50 mM Fe^{2+} and (◊) photoelectro-Fenton (PEF) with 0.50 mM Fe^{2+} under irradiation with a 4 W UVA lamp.

3.0 and 300 mA upon addition of 0.10-1.50 mM Fe^{2+}. As can be seen in Fig. S1a, a quicker ST decay resulted from increasing the initial Fe^{2+} concentration, needing 270, 120, 75 and 60 min for total ST removal at 0.10, 0.50, 1.00 and 1.50 mM Fe^{2+}, respectively. Again, two consecutive regions agreeing with a pseudo-first-order kinetics, were found (see the inset of Fig. S1a). The decay in the first region was much more rapid than in the second one, as confirmed from k_{app} values in Table 1. Note that, in the first region, the abatement of the herbicide at 1.50 mM Fe^{2+} was slower than that at 1.00 mM, which can be related to the decay of available ·OH in the bulk by its consumption in the parasitic reaction between hydroxyl radicals and Fe^{2+} species [29,30]. The kinetics at the lowest Fe^{2+} concentration was quite similar to that of EO-H_2O_2, as confirmed from the analogous k_{app} values obtained (Table 1).

Fig. S1b shows that the mineralization attained at 9 h was 83% at 0.10 mM Fe^{2+}, and up to 95% at 0.50–1.50 mM. Although slightly quicker TOC abatements can be seen as the Fe^{2+} content was increased from 0.50 mM, the accumulation of refractory complexes formed between Fe(III) and some byproducts like short-chain carboxylic acids caused the deceleration of the degradation at long treatment time, eventually ending in similar abatements. The inset shows the MCE values along the electrolyses, which were somewhat greater at high Fe^{2+} concentration during the first hours, but tended to become equal at the end of the treatments.

3.4. Effect of initial ST concentration on the EF process

The influence of the initial ST content on the EF performance was studied by treating solutions with concentrations between 0.14 and 0.56 mM in 0.050 M Na_2SO_4 with 0.50 mM Fe^{2+} at pH 3.0 and 300 mA. Fig. S2a highlights a total ST removal in all cases, requiring 60, 105 and 360 min upon gradual ST increase. This agrees with the expected analogous concentration of hydroxyl radicals available in the three cases, which is then used for reacting with a gradually larger number of ST molecules. Two different slopes appeared upon kinetic analysis of consecutive regions (see inset panel of Fig. S2a and k_{app} values in Table 1), as explained above. Quite similar normalized TOC removals were obtained regardless of the initial ST concentration, as shown in Fig. S2b, achieving 92%, 96% and 88% for 0.14, 0.28 and 0.56 mM, respectively. The MCE of the EF treatment was then enhanced as the ST content was raised (see the inset panel of Fig. S2b), reaching 4.8% for 0.56 mM ST and 1.3% for 0.14 mM ST after 9 h. This behavior suggests that parasitic reactions (8)–(11) were given to a lower extent since hydroxyl radicals and H_2O_2 were able to encounter organic molecules more easily, which is very positive whenever concentrated effluents containing this herbicide have to be treated by EF process.

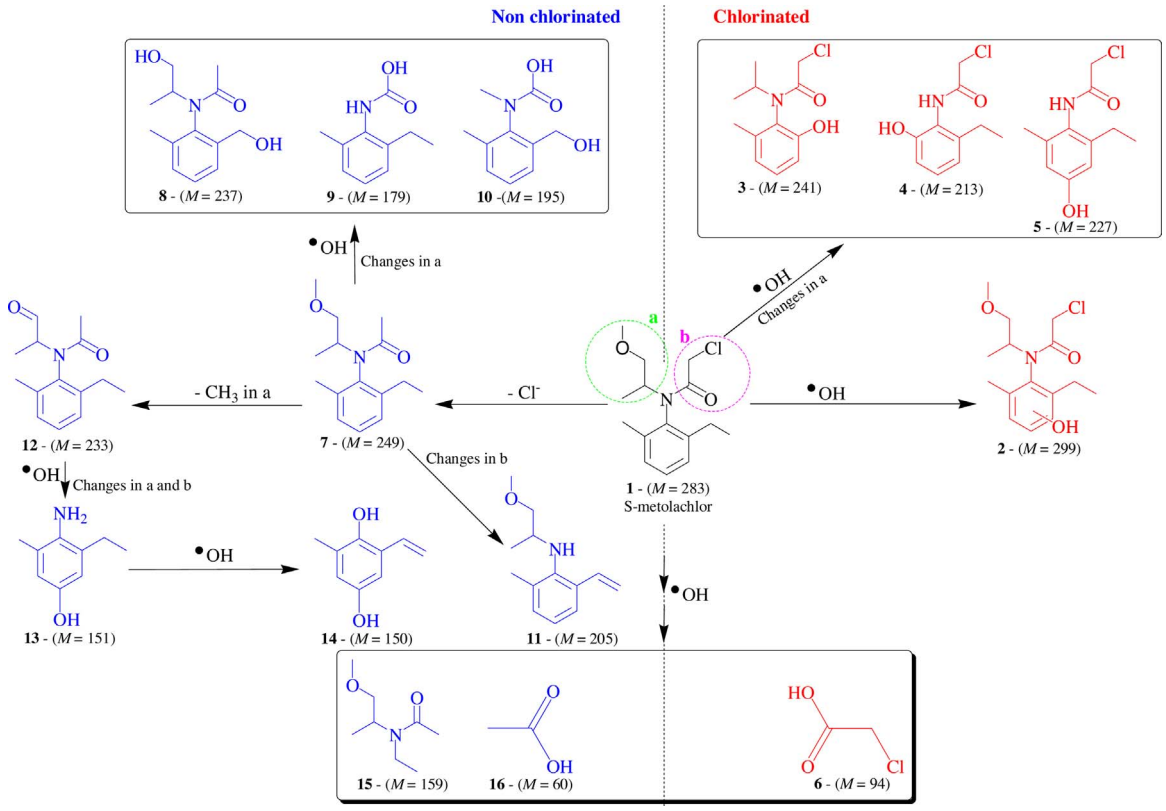

Fig. 4. Scheme of the possible routes for S-metolachlor degradation proposed from all the by-products identified by GC–MS.

3.5. Degradation of S-metolachlor by PEF

Aiming to promote a faster degradation of ST, the performance of EO-H_2O_2 and EF treatments of 0.28 mM ST solutions with 0.050 M Na_2SO_4 at pH 3.0 and 300 mA was compared with that of PEF using 0.50 mM Fe^{2+} and a 4 W UVA lamp. Fig. 3 informs about the remarkable superiority of PEF under those comparable conditions, being especially substantial for the herbicide concentration decay. ST was totally abated after 240, 75 and 45 min by EO-H_2O_2, EF and PEF, respectively, as shown in Fig. 3a. This means that the UVA radiation was quite effective for ensuring the regeneration of Fe^{2+} from photo-Fenton reaction (5), as confirmed in the inset. Two consecutive pseudo-first-order kinetics were also obtained in PEF, as in EF, although with a more pronounced slope of the straight lines in the two regions (see k_{app} values in Table 1). This can be related to the quicker ST destruction in PEF by the action of additional ·OH induced by reaction (5), which causes the faster formation of Fe(III)-ST complexes with the consequent appearance of the inflection point at shorter time compared to EF. These results agree with those reported recently for the inseticide propoxur, which conforms the formation of Fe(III) complexes [20]. The oxidation ability of the EAOPs then increased in the order EO-H_2O_2 < EF < PEF. In contrast, the TOC decay attained at 9 h was similar in the three processes, with around 95% of mineralization (see Fig. 3b), which can be explained by the great persistence of final by-products, either free or complexed with Fe(III). These species are preeminently destroyed by BDD(·OH), presenting a much slower kinetic constant with ·OH in the bulk. The similar MCE values achieved during the three treatments after some initial minutes (inset of Fig. 3b) confirm the formation of refractory compounds and/or complexes.

3.6. Main degradation routes

Based on the byproducts identified by GC–MS during the treatment of ST solutions by the three EAOPs, the possible degradation pathways are proposed in Fig. 4. Two sets of compounds were found, including chlorinated and non-chlorinated compounds. The first set appeared upon hydroxylation of ST (**1**), which yielded **2** from the single attack of ·OH/BDD(·OH) onto the benzene ring or **3**, **4** and **5** if concomitant changes in the $-NCH(CH_3)CH_2OCH_3$ group occurred. All these by-products maintained the initial $-COCH_2Cl$ group, but the attack of hydroxyl radicals onto the carbonyl group of these compounds favored the formation of chloracetic acid (**6**), which is known to be a very refractory molecule to ·OH formed from Fenton's reaction (3) [39]. The second set of compounds was formed upon Cl^- release to form dechlorinated ST (**7**). Hydroxylation of the ethyl group bonded to the aromatic ring or the side group *a*, with or without changes in *b*, yielded **8**, **9** and **10**. Alternatively, changes in the side group *b* yielded compound **11**, whose ethyl group is also modified. Demethylation of **7** explains the formation of **12**, whereas subsequent hydroxylation in *para* position yielded the aminophenol **13**. Hydroquinone **14** appeared upon attack of hydroxyl radicals on the amino position of the aromatic ring. Finally, the cleavage of the previous aromatic byproducts ended in aliphatic compound **15** along with acetic acid (**16**). Nitrogen atom contained in ST or any of its byproducts was mainly accumulated as ammonium ion, as described in reaction (8).

4. Conclusions

The application of EAOPs to treat aqueous solutions contaminated with ST was thoroughly evaluated. It has been shown that the rate of degradation and mineralization for solutions with 0.28 mM ST treated by EO-H_2O_2 is slightly higher at pH 3.0. However, at that pH, the performance of EF was much better thanks to the formation of hydroxyl radicals in the bulk, which overcome the mass transport limitations that are typical in EO. The decay kinetics in all the EF trials presented two well-defined regions, being the second one much slower than the first, which is associated to the formation of Fe(III)-ST complexes that hamper the Fe^{2+} regeneration. The increase in current and Fe^{2+}

concentration was beneficial since the treatments were accelerated, but lower MCE values were obtained. EF was more efficient at higher initial ST concentrations due to the minimization of parasitic reactions. In PEF treatment, which also presented two regions related to pseudo-first-order kinetics, the abatement of ST was clearly upgraded, although the degree of mineralization by EO-H_2O_2, EF and PEF was quite similar because complexed and uncomplexed byproducts turned out to be refractory. Up to 15 byproducts, including chlorinated and non-chlorinated ones, have been identified by GC–MS.

Acknowledgments

The authors thank financial support from Brazilian funding agencies: Fundação de Apoio ao Desenvolvimento do Ensino, Ciência e Tecnologia do Estado de Mato Grosso do Sul (FUNDECT-MS), Pró-Reitoria de Pesquisa e Pós-Graduação da Universidade Federal de Mato Grosso do Sul (PROPP-UFMS), Coordenação de Aperfeiçoamento de Pessoal de Nível Superior (CAPES), and Conselho Nacional de Desenvolvimento Científico e Tecnológico (CNPQ). Financial support from project CTQ2016-78616-R (AEI/FEDER, EU) is also acknowledged.

Appendix A. Supplementary data

Supplementary data associated with this article can be found, in the online version, at http://dx.doi.org/10.1016/j.cattod.2017.10.026.

References

[1] A. De, R. Bose, A. Kumar, S. Mozumdar, Targeted Delivery of Pesticides Using Biodegradable Polymeric Nanoparticles, Springer, New Delhi, 2014.
[2] P.J. O'Connell, C.T. Harms, J.R.F. Allen, Metolachlor, S-metolachlor and their role within sustainable weed-management, Crop Prot. 17 (1998) 207–212.
[3] United States Environmental Protection Agency, Re-registration Eligibility Decision (RED): Metolachlor, 1995. Available at: https://archive.epa.gov/pesticides/reregistration/web/pdf/0001.pdf Accessed in 01 May 2017.
[4] World Health Organization, Guidelines for Drinking-Water Quality, 4th ed., (2011) (Geneva) Available at: http://apps.who.int/iris/bitstream/10665/44584/1/9789241548151_eng.pdf Accessed in 01 May, 2017.
[5] L. Rivard, Environmental Fate of Metolachlor, (2003) (Available at: http://cdpr.ca.gov/docs/emon/pubs/fatememo/metolachlor.pdf Accessed in 01 May 2017).
[6] Agência Nacional de Vigilância Sanitária. Monografias Autorizadas: S13-S-metolacloro, 2014. Available at: http://portal.anvisa.gov.br/documents/111215/117782/S13%2BS%2BMetolacloro%2Batual.pdf/964f38ac-f7c9-4a57-b1e0-1c99ee5f939b Accessed in 01 May 2017.
[7] M. Thakkar, V. Randhawa, L. Wei, Comparative responses of two species of marine phytoplankton to metolachlor exposure, Aquat. Toxicol. 126 (2013) 198–206.
[8] C. Quintaneiro, D. Patrício, S.C. Novais, A.M.V.M. Soares, M.S. Monteiro, Endocrine and physiological effects of linuron and S-metolachlor in zebrafish developing embryos, Sci. Total Environ. 586 (2017) 390–400.
[9] H. Mai, B. Morin, P. Pardon, P. Gonzalez, H. Budzinski, J. Cachot, Environmental concentrations of irgarol diuron and S-metolachlor induce deleterious effects on gametes and embryos of the Pacific oyster, *Crassostrea gigas*, Mar. Environ. Res. 89 (2013) 1–8.
[10] S. Hartnett, S. Musah, K.R. Dhanwada, Cellular effects of metolachlor exposure on human liver (HepG2) cells, Chemosphere 90 (2013) 1258–1266.
[11] V.A. Sakkas, I.M. Arabatzis, I.K. Konstantinou, A.D. Dimou, T.A. Albanis, P. Falaras, Metolachlor photocatalytic degradation using TiO_2 photocatalysts, Appl. Catal. B: Environ. 49 (2004) 195–205.
[12] P.L. Huston, J.J. Pignatello, Degradation of selected pesticide active ingredients and commercial formulations in water by the photo-assisted Fenton reaction, Water Res. 33 (1999) 1238–1246.
[13] J.J. Pignatello, Y. Sun, Complete oxidation of metolachlor and methyl parathion in water by the photoassisted Fenton reaction, Water Res. 29 (1995) 1837–1844.
[14] K. Pratap, A.T. Lemley, Fenton electrochemical treatment of aqueous atrazine and metolachlor, J. Agric. Food Chem. 46 (1998) 3285–3291.
[15] A. Da Pozzo, C. Merli, I. Sirés, J.A. Garrido, R.M. Rodríguez, E. Brillas, Removal of the herbicide amitrole from water by anodic oxidation and electro-Fenton, Environ. Chem. Lett. 3 (2005) 7–11.
[16] E. Brillas, M.A. Baños, M. Skoumal, P.L. Cabot, J.A. Garrido, R.M. Rodríguez, Degradation of the herbicide 2,4-DP by anodic oxidation, electro-Fenton and photoelectro-Fenton using platinum and boron-doped diamond anodes, Chemosphere 68 (2007) 199–209.
[17] A. Kesraoui-Abdesalem, N. Oturan, N. Bellakhal, M. Dachraoui, M.A. Oturan, Experimental design methodology applied to electro-Fenton treatment for degradation of herbicide chlortoluron, Appl. Catal. B: Environ. 78 (2008) 334–341.
[18] M.A. Rodrigo, N. Oturan, M.A. Oturan, Electrochemically assisted remediation of pesticides in soils and water: a review, Chem. Rev. 114 (2014) 8720–8745.
[19] P.A. Diaw, N. Oturan, M.D. Gaye-Seye, A. Coly, A. Tine, J.-J. Aaron, M.A. Oturan, Oxidative degradation and mineralization of the phenylurea herbicide fluometuron in aqueous media by the electro-Fenton process, Sep. Purif. Technol. 186 (2017) 197–206.
[20] D.R.V. Guelfi, F. Gozzi, I. Sirés, E. Brillas, A. Machulek Jr., S.C. de Oliveira, Degradation of the insecticide propoxur by electrochemical advanced oxidation processes using a boron-doped diamond/air-diffusion cell, Environ. Sci. Pollut. Res. 24 (2017) 6083–6095.
[21] C. Flox, J.A. Garrido, R.M. Rodríguez, P.L. Cabot, F. Centellas, C. Arias, E. Brillas, Mineralization of herbicide mecoprop by photoelectro-Fenton with UVA and solar light, Catal. Today 129 (2007) 29–36.
[22] F. Gozzi, I. Sirés, A. Thiam, S.C. de Oliveira, A. Machulek Jr., E. Brillas, Treatment of single and mixed pesticide formulations by solar photoelectro-Fenton using a flow plant, Chem. Eng. J. 310 (2017) 503–513.
[23] A. El-Ghenymy, F. Centellas, R.M. Rodríguez, P.L. Cabot, J.A. Garrido, I. Sirés, E. Brillas, Comparative use of anodic oxidation, electro-Fenton and photoelectro-Fenton with Pt or boron-doped diamond anode to decolorize and mineralize Malachite Green oxalate dye, Electrochim. Acta 182 (2015) 247–256.
[24] A. Thiam, I. Sirés, J.A. Garrido, R.M. Rodríguez, E. Brillas, Decolorization and mineralization of Allura Red AC aqueous solutions by electrochemical advanced oxidation processes, J. Hazard. Mater. 290 (2015) 34–42.
[25] A.J. Bañuelos, O. García-Rodríguez, A. El-Ghenymy, F.J. Rodríguez-Valadez, L.A. Godínez, E. Brillas, Advanced oxidation treatment of malachite green dye using a low cost carbon-felt air-diffusion cathode, J. Environ. Chem. Eng. 4 (2016) 2066–2075.
[26] A. Bedolla-Guzman, I. Sirés, A. Thiam, J.M. Peralta-Hernández, S. Gutiérrez-Granados, E. Brillas, Application of anodic oxidation, electro-Fenton and UVA photoelectro-Fenton to decolorize and mineralize acidic solutions of Reactive Yellow 160 azo dye, Electrochim. Acta 206 (2016) 307–316.
[27] G. Coria, I. Sirés, E. Brillas, J.L. Nava, Influence of the anode material on the degradation of naproxen by Fenton-based electrochemical processes, Chem. Eng. J. 304 (2016) 817–825.
[28] J.R. Steter, E. Brillas, I. Sirés, On the selection of the anode material for the electrochemical removal of methylparaben from different aqueous media, Electrochim. Acta 222 (2016) 1464–1474.
[29] E. Brillas, I. Sirés, M.A. Oturan, Electro-Fenton process and related electrochemical technologies based on Fenton's reaction chemistry, Chem. Rev. 109 (2009) 6570–6631.
[30] I. Sirés, E. Brillas, M.A. Oturan, M.A. Rodrigo, M. Panizza, Electrochemical advanced oxidation processes: today and tomorrow. A review, Environ. Sci. Pollut. Res. 21 (2014) 8336–8367.
[31] I. Sirés, E. Brillas, Remediation of water pollution caused by pharmaceutical residues based on electrochemical separation and degradation technologies: a review, Environ. Int. 40 (2012) 212–229.
[32] C.A. Martínez-Huitle, M.A. Rodrigo, I. Sirés, O. Scialdone, Single and coupled electrochemical processes and reactors for the abatement of organic water pollutants: a critical review, Chem. Rev. 115 (2015) 13362–13407.
[33] C.G. Hatchard, C.A. Parker, A new sensitive chemical actinometer – II. Potassium ferrioxalate as a standard chemical actinometer, Proc. R. Soc. A 235 (1956) 518–536.
[34] Environmental Protection Agency – SW 846, Testing Methods for Evaluating Solid Wastes: Physical/Chemical Methods, 3rd, (2015) (final update V).
[35] American Public Health Association, American Works Association, Water Environment Federation, Standard Methods for the Examination of Water and Wastewater, 22nd, (2012) (Washington, DC).
[36] E. Guinea, C. Arias, P.L. Cabot, J.A. Garrido, R.M. Rodríguez, F. Centellas, E. Brillas, Mineralization of salicylic acid in acidic aqueous medium by electrochemical advanced oxidation processes using platinum and boron-doped diamond as anode and cathodically generated hydrogen peroxide, Water Res. 42 (2008) 499–511.
[37] E. Brillas, M.A. Baños, J.A. Garrido, Mineralization of herbicide 3,6-dichloro-2-methoxybenzoic acid in aqueous medium by anodic oxidation, electro-Fenton and photoelectro-Fenton, Electrochim. Acta 48 (2003) 1697–1705.
[38] T.A. Enache, A.M. Chiorcea-Paquim, O. Fatibello-Filho, A.M. Oliveira-Brett, Hydroxyl radicals electrochemically generated in situ on a boron-doped diamond electrode, Electrochem. Commun. 11 (2009) 1342–1345.
[39] S. Randazzo, O. Scialdone, E. Brillas, I. Sirés, Comparative electrochemical treatments of two chlorinated aliphatic hydrocarbons. Time course of the main reaction by-products, J. Hazard. Mater. 192 (2011) 1555–1564.